

Overlayer Structure and Kinetic Behavior of Benzene on Palladium(111)

W. T. Tysoe*

Department of Chemistry and Laboratory for Surface Studies, University of Wisconsin, Milwaukee, Wisconsin 53211

R. M. Ormerod† and R. M. Lambert

Department of Chemistry, University of Cambridge, Cambridge, CB2 1EW, UK

G. Zgrablich and A. Ramirez-Cuesta

Centro Regional de Estudios Avanzados (CREA) Gobierno de la Provincia de San Luis and Instituto de Investigaciones en Tecnología Química (INTEQUI), Casilla de Correo 290, 5700 San Luis, Argentina

Received: November 3, 1992; In Final Form: January 5, 1993

The structural and kinetic properties of benzene on Pd(111) are studied at 200 K using temperature-programmed desorption. Benzene completely thermally decomposes on Pd(111) for coverages below 0.05 (where coverages are referred to the number of exposed palladium atoms on the (111) surface) but desorbs molecularly in two distinct states at higher coverages. This behavior is explained by invoking a repulsive molecular interaction between adjacent adsorbed benzenes and confirmed using Monte Carlo simulations of the thermal desorption spectra. Benzene adsorbs onto palladium with an initial sticking probability of unity, the overlayer saturating at a benzene coverage of 0.13. Further benzene adsorbs but with a much lower sticking coefficient (0.03) up to an ultimate saturation coverage of ~ 0.22 , the additional benzene desorbing at low temperature (~ 280 K). This, along with results of experiments where the benzene overlayer is compressed using NO, indicates that this state is due to the presence of a tilted benzene layer.

Introduction

Cyclization of acetylene to benzene occurs efficiently at low temperatures (< 200 K) on the (111) face of palladium.¹⁻³ The overall reaction pathway has been established:^{4,5} flat-lying acetylene molecules couple to form a C₄ intermediate⁶ which undergoes cyclization with a third acetylene molecule to yield benzene. This mechanism also successfully accounts for the formation of thiophene,⁷ furan,⁸ and butadiene⁹ in the presence of sulfur, oxygen, and hydrogen atoms, respectively. In the case of benzene production, the rate-limiting kinetics of product desorption are interesting and unusual; in a temperature-programmed reaction experiment, benzene evolution into the gas phase occurs in two distinct and widely separated stages yielding desorption maxima at ~ 280 and ~ 520 K. We have argued that this behavior is due to the desorption of tilted (weakly adsorbed) and flat-lying (more strongly adsorbed) benzene molecules respectively, the transition between the two species being driven by a relief of the surface crowding by the conversion of a portion of the adsorbed hydrocarbons to vinylidene species. Near-edge X-ray absorption fine structure (NEXAFS) observations on dense benzene overlayers on Pd(111)¹⁰ demonstrate that the molecule is indeed tilted at high surface coverages. The results of experiments¹¹ involving compression of the reacting acetylene phase by inert spectator molecules (nitric oxide) are in excellent accord with the tilted/flat hypothesis. Likewise, the acetylene \rightarrow benzene activity of Pd(111) films on a Au(111) substrate provides strong support for this view of the desorption kinetics of reactively formed benzene.¹²

The present paper reports on the adsorption/desorption kinetics of benzene itself on Pd(111). A principal aim is to address directly the effect of overlayer density and adsorbate geometry on the desorption process: as noted above, desorption is rate limiting in the synthesis of benzene from acetylene. Monte Carlo simulations

of the thermal desorption spectra of benzene and hydrogen resulting from benzene decomposition suggest that the heat of adsorption of benzene on Pd(111) is 101 kJ/mol and that there is a strong repulsive lateral interaction between neighboring benzene molecules of 6.5 kJ/mol. These simulations also successfully explain the observed transition from benzene decomposition to carbon and hydrogen at low coverages ($\theta < 0.05$) to molecular desorption for $\theta > 0.05$ as well as the shape of the benzene desorption states.

Experimental Methods

Experiments were carried out in an apparatus that has been described in detail elsewhere.¹³ The stainless steel ultrahigh-vacuum chamber operated at a base pressure of 2×10^{-11} Torr; it contained a four-grid retarding field analyzer (RFA) for LEED/Auger observations and a quadrupole mass spectrometer for gas analysis and thermal desorption measurements. The computer-multiplexed mass spectrometer allowed up to 16 different ion signals to be monitored simultaneously. Gases were introduced into the chamber either via a variable leak or by means of a capillary array dosing source. Calibration of the dosing source for benzene flux was achieved by carrying out the appropriate control experiments involving comparisons of benzene uptake achieved with the source and by back-filling the chamber. The capillary array doser was also used for measuring the coverage dependence of sticking probability following the method of King and Wells;^{14,1} the benzene signal due to scattered molecules was monitored as a function of time after rapidly moving the clean sample in front of the capillary array so as to intercept the benzene flux.

The palladium single crystal was attached to 2-mm Mo rods by means of 0.25-mm Ta wires and mounted on an XYZ rotary motion feedthrough. It could be resistively heated and also be cooled by being brought into thermal contact with a moveable liquid nitrogen-filled reservoir. Specimen cleaning was achieved by heating the sample to ~ 800 K in a pressure of $\sim 1 \times 10^{-6}$ Torr

* To whom correspondence should be addressed.

† Present address: Department of Chemistry, University of Keele, Keele, Staffordshire, ST5 5BG, UK

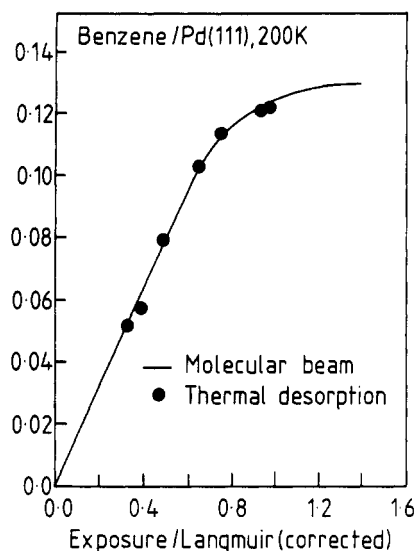


Figure 1. Benzene coverage plotted as a function of exposure for adsorption at a sample temperature of 200 K obtained using the capillary array dosing source (solid line) up to an exposure of 1.6 langmuirs. Plotted also on this curve are the total benzene thermal desorption yields obtained from the areas of the thermal desorption spectra displayed in Figure 3 (●). These points have been shifted to take account of the benzene that thermally decomposes to hydrogen at low coverages. Exposures have been corrected for the ionization gauge sensitivity.

of oxygen introduced via the dosing source. Subsurface carbon contamination was particularly troublesome, and it was found that a sensitive index of cleanliness was to saturate the surface with oxygen and monitor the resulting desorption spectra. Initially only CO desorbed; subsequently some O₂ desorption was observed along with CO; finally only O₂ desorbed with no trace of any CO. Benzene (Aldrich, 99.9%) was purified by several freeze-pump-thaw cycles, the purity of the gas being monitored using mass spectrometry. Gas exposures have been corrected to take account of ionization gauge sensitivity factors.

Results

Benzene adsorbs rapidly on Pd(111) at 200 K, the only products evolved during subsequent heating being hydrogen (due to some benzene decomposition) and benzene itself. Adsorption kinetic data collected using the capillary array doser for benzene obtained at 200 K are displayed in Figure 1 (solid line) as a plot of coverage (where benzene coverages are referred to the number density of palladium atoms on the (111) surface) versus benzene exposure. Benzene exposures are corrected for ionization gauge sensitivity using a value of 5.7 for the sensitivity factor.¹⁵ These results were obtained by integrating the sticking probability (i.e., pressure drop) versus exposure data obtained at 200 K by the King and Wells method.^{14,1} The initial sticking probability measured directly from the slope of this curve and also by comparing the initial pressure drop observed with benzene with the corresponding results of a similar experiment for acetylene (initial sticking probability of unity¹) indicates that the initial sticking probability is constant at 1.0 ± 0.1 up to a coverage of ~ 0.1 and decreases at higher coverages. These data also yield a value of 0.13 ± 0.01 for the saturation coverage of benzene at 200 K.

Figure 2 shows 2 amu (H₂) thermal desorption spectra as a function of benzene coverage; the benzene coverages obtained using the data in Figure 1 are indicated adjacent to each spectrum. For low benzene coverages ($0 < \theta < 0.04$), the H₂ spectra exhibit a single peak centered at ~ 560 K. This temperature is significantly higher than that characteristic of H₂ desorption from a hydrogen overlayer on clean palladium (peak temperature ~ 350 K) suggesting that in the present case hydrogen evolution is controlled by the kinetics of benzene dehydrogenation, rather than being desorption rate limited. For higher benzene coverages

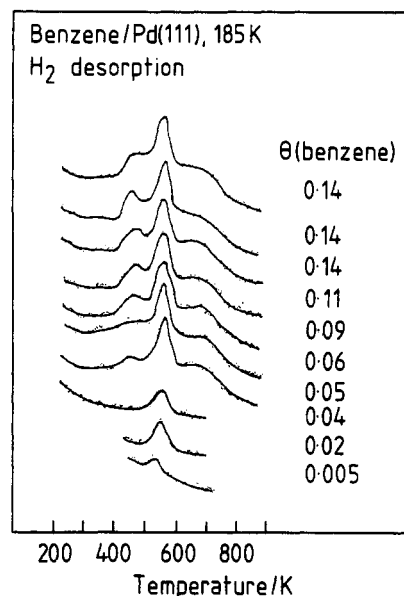


Figure 2. The 2 amu (H₂) thermal desorption spectra obtained as a function of coverage following adsorption of benzene on palladium at 195 K. Benzene coverages are marked adjacent to their corresponding spectra, which were collected using a heating rate of 8 K/s.

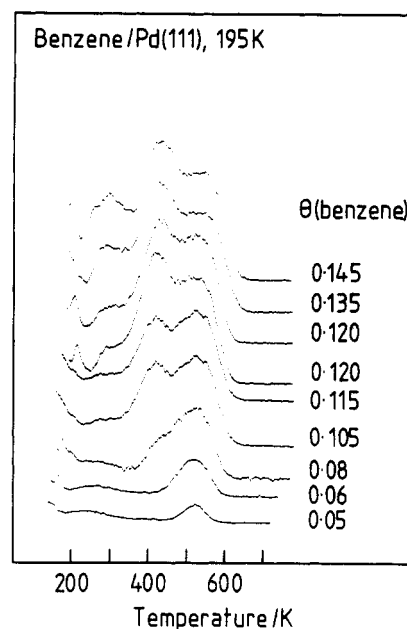


Figure 3. The 78 amu (benzene) thermal desorption spectra obtained as a function of coverage following adsorption of benzene on palladium at 195 K showing the evolution of the β and γ states with coverage and the onset of the α state. Benzene coverages are marked adjacent to their corresponding spectra which were collected using a heating rate of 8 K/s.

($\theta \geq 0.04$), the 560 K H₂ peak is superimposed on a broad background extending from 400 to 750 K; the H₂ desorption yield saturates at a benzene coverage of 0.05.

The establishment of reliable values for benzene coverages is an important matter for the discussion that follows—especially since the C(KLL) Auger signal cannot be used due to overlap with the strong Pd(MNN) signal. In addition to the methods employed above, the hydrogen desorption yield from benzene overlayers with $\theta < 0.05$ were compared with the desorption yield from a hydrogen overlayer assuming $\theta_{\text{sat}}(\text{H}) = 1.0$ on Pd(111).¹⁶ This yields values that are within 10% of those reported above.

Corresponding benzene desorption spectra (78 amu) as a function of benzene coverage are shown in Figures 3 and 4. Again, benzene coverages derived from the data of Figure 1 are indicated adjacent to each spectrum. Note that no benzene desorption

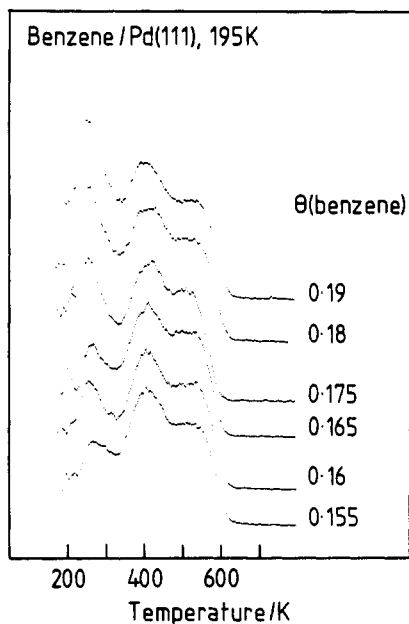


Figure 4. The 78 amu (benzene) thermal desorption spectra obtained as a function of coverage following adsorption of benzene on palladium at 195 K showing the evolution of the α state with exposure. Benzene coverages are marked adjacent to their corresponding spectra which were collected using a heating rate of 8 K/s.

occurs for $\theta \leq 0.05$, indicating that the molecule undergoes decomposition to carbon and hydrogen in this low-coverage regime; this accords quantitatively with the H_2 data reported above. For $\theta \geq 0.05$, benzene desorption occurs as a single broad peak centered at 520 K (γ state). Simple first-order analysis¹⁷ of the desorption kinetics using a preexponential factor of $1 \times 10^{13} \text{ s}^{-1}$ yields an estimate of $\sim 130 \text{ kJ/mol}$ for the desorption energy associated with this state. The intensity of this peak saturates at $\theta = 0.09$ and a new feature centered at 380 K develops at higher coverages (β state). The estimated desorption activation energy associated with this state $\sim 95 \text{ kJ/mol}$. The β state intensity saturates at $\theta = 0.13$ which corresponds to the apparent saturation benzene uptake measured using the capillary array source to follow the adsorption kinetics (Figure 1). The small feature evident at $\sim 200 \text{ K}$ in some of these spectra is due to desorption from sample supports.

A strong check may be obtained on the consistency of the adsorption and desorption data by comparing the benzene uptake as measured by the two methods, as follows. Relative benzene coverages are readily obtained from the total benzene desorption yield in the β and γ states in the spectra shown in Figure 3. These desorption derived coverages are uniformly incremented by 0.05 to take account of the thermal decomposition that occurs at low coverage (Figure 2) and then scaled so that they correspond at saturation. The two data sets should yield identical coverage versus exposure curves. This is illustrated in Figure 1 (●) from which it is apparent that the two sets of data are indeed consistent; it also confirms that no species other than benzene and hydrogen desorb.

At higher coverages ($\theta > 0.13$), a third peak appears in the benzene desorption spectra (α state, Figures 3 and 4). The position of this peak ($\sim 280 \text{ K}$) agrees well with that of the low-temperature benzene peak, which appears in the temperature-programmed synthesis of benzene from acetylene on Pd(111).¹⁻⁴ The intensity of this feature grows relatively slowly with increasing exposure, and Figure 5 shows the benzene desorption yield (derived from the data in Figures 3 and 4) as a function of exposure, including the high-exposure regime, for a sample temperature of 185 K. These data show the initial rapid uptake of benzene detected by monitoring the adsorption kinetics (Figure 1). However, they also reveal an additional slow increase in benzene uptake for

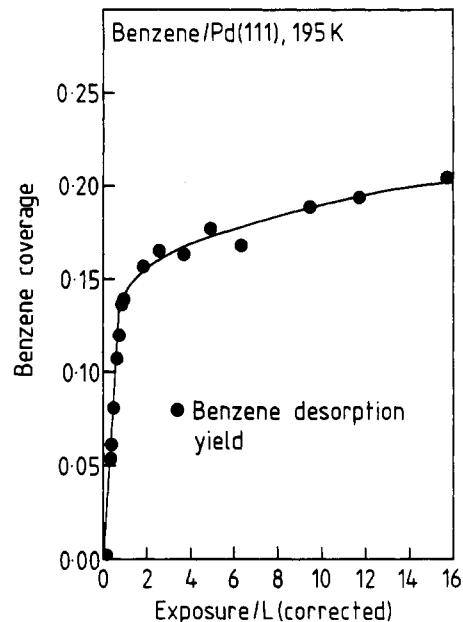


Figure 5. Plot of the benzene coverage measured from the thermal desorption yield obtained from the data shown in Figures 3 and 4 up to an exposure of 16 langmuirs showing population of the 280 K (α) thermal desorption state.

exposures > 1 langmuirs corresponding to population of the $\sim 280 \text{ K}$ α state. Given the initial sticking probability of benzene (1.0 ± 0.1) we may calculate that the sticking probability into this state is $\sim 0.030 \pm 0.005$. This relatively small value accounts for our inability to observe population of the α state using the King and Wells method at long impingement times due to limitations of the signal-to-noise ratio. The α peak attains its maximum intensity at a benzene coverage of $\theta = 0.21 \pm 0.02$, in good agreement with coverage measurements made by XPS on a saturated benzene layer at 200 K, where a value of $\theta \sim 0.24$ was found.¹⁰ A significantly smaller population of the α state was observed for adsorption of benzene on Pd(111) for a sample temperature of 100 K.⁵ Rather the formation of a condensed multilayer was noted in that case indicating that the population of the α state is an activated process.

Discussion

Our principal purpose is to account for the four stages of benzene interaction with the Pd(111) surface: dehydrogenation/decomposition followed by successive population of the γ , β , and α states. The implications of these findings for the kinetics of benzene synthesis from acetylene on Pd(111) will also be explored. We shall argue in favor of the following model: (a) for $\theta < 0.05$ the surface is covered with flat-lying benzene molecules which have no nearest-neighbor benzenes; on heating these undergo decomposition yielding gaseous hydrogen and surface carbon.

(b) For $0.05 < \theta < 0.09$ any given flat-lying benzene molecule will begin to accumulate nearest neighbor molecules; decomposition is inhibited because of repulsive interactions between nearest neighbors which kinetically facilitates molecular desorption relative to decomposition and desorption of the γ state is observed.

(c) For $0.09 < \theta < 0.14$ any given benzene molecule begins to acquire further nearest neighbors; the increased lateral interactions in the overlayer lead to the appearance of the β state feature in the desorption spectrum. This process culminates at $\theta = 0.14$, when every flat-lying benzene molecule is surrounded by six nearest neighbors and the intensity of the β -state reaches its maximum value. This coverage corresponds to the maximum amount of benzene that can be accommodated in a flat-lying orientation.

(d) For $0.14 < \theta < 0.22$ adsorption into the dense layer of flat-lying molecules becomes an activated process; additional

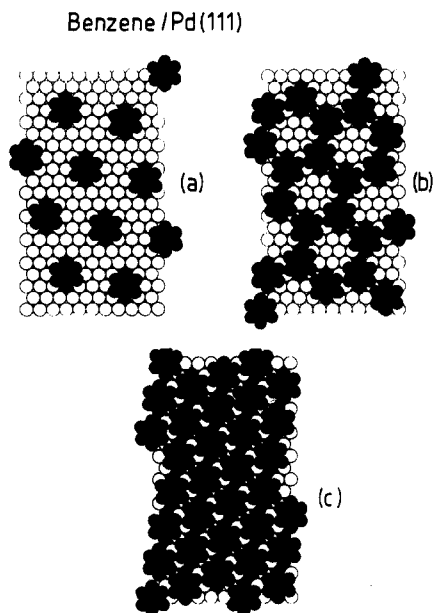


Figure 6. Proposed structural models for the adsorption of benzene on the palladium(111) surface corresponding to benzene coverages of (a) 0.05, (b) 0.095, and (c) 0.14.

molecules are accommodated by tilting of the adsorbed species. This reorientation drastically weakens the adsorbate-metal interaction and leads to the appearance of the α desorption feature.

A number of studies using a variety of methods have shown that benzene adsorbs on (111) surfaces of the group VIII metals in a flat-lying conformation; i.e., with the molecular plane parallel to the surface.¹⁸⁻²⁹ In some cases, most notably on Pd(111)²³ and Ir(111),²⁹ Kekulé distortions have been found such that molecular symmetry is reduced to C_3 . On Pt(111) adsorption onto the 2-fold bridge site has been proposed.²⁴ Our proposed model is supported by excellent agreement between the experimental results and plausible structural models for the various stages of overlayer desorption; it is also in accord with our Monte Carlo calculations that are described below.

Flat-Lying Benzene. Figure 6a schematically depicts the surface at the point where the γ -state desorption is just about to begin. It is important to note that the benzene molecules have been drawn using the appropriate van der Waals' radii. The insertion of additional flat-lying benzene molecules into this layer removes bare metal sites (which are presumably necessary for C-H bond cleavage). In addition, repulsive interactions between adjacent benzenes permits the onset of desorption without decomposition. The structure in Figure 6a corresponds to $\theta = 0.05$ which is in very good agreement with the experimental observation that the γ -state desorption commences at $\theta \geq 0.05$ with complete decomposition occurring at lower coverages. Figure 6b shows the point at which the γ state saturates. Here, every benzene has three nearest neighbors; addition of further benzene sharply increases the amount of repulsive interaction in the overlayer and leads to the appearance of the β peak. On this basis, the predicted coverage at which β desorption should appear is 0.09, again in very good agreement with the experimentally observed value.

Figure 6c shows the Pd(111) surface saturated with flat-lying benzene molecules, again depicted according to their van der Waals' radii. The theoretical saturation coverage is $1/7 = 0.14$. This value corresponds very well to the experimentally determined point at which the β state desorption saturates (0.13, Figure 1).

Monte Carlo simulations of the benzene and hydrogen thermal desorption spectra (Figures 2 and 3) were carried out in order to establish whether our structural model is able to account in a quantitative manner for the observed desorption kinetics for the flat-lying benzene state, in particular the marked switch from

complete benzene decomposition for $\theta < 0.05$ to molecular desorption for $\theta > 0.05$. Simulations of temperature programmed desorption and reaction spectra using Monte Carlo techniques have been described in detail elsewhere.^{30,31} The salient features only will be described here as they pertain to benzene on palladium. Following the model described in refs 30 and 31, the simulation uses a triangular lattice of N sites (where N is typically 10^4), each site having six nearest neighbors (NN). A particular chemisorbed benzene molecule at any site labeled i is allowed to undergo one of two processes; decomposition into carbon and hydrogen or desorption.

The activation energy for desorption E_d is given by

$$E_d = E_{\text{ads}} + W \sum_{j(\text{NN}) \text{ to } i} s_j \quad (1)$$

where E_{ads} is the adsorption energy at site i and W is the NN interaction energy between neighboring chemisorbed benzenes (taken to be positive for an attractive interaction). s_j is the occupation number of site j taken to be zero for a vacant site and unity for an occupied one. The summation is made over all sites j onto which NN molecules can adsorb. The probability P_d that a benzene molecule can desorb in a temperature interval between T and $T + \Delta T$ is given by

$$P_d = \nu_d(\Delta T/\nu) \exp(-E_d/RT) \quad (2)$$

where ν_d is the desorption preexponential factor and ν the experimental heating rate (8 K/s).

It is assumed that chemisorbed benzene can only decompose when vacant sites are available around the i th molecule to accommodate the hydrogen so that the presence of nearest-neighbor benzenes will also inhibit decomposition. This can be taken into account by writing the reaction activation energy E_r as

$$E_r = E_r^0 + V \sum_{j(\text{NN}) \text{ to } i} s_j \quad (3)$$

where E_r^0 is the reaction activation energy at vanishingly low coverage and V is an interaction energy such that positive values of V inhibit reaction. The reaction probability P_r in a temperature range between T and $T + \Delta T$ is given as

$$P_r = \nu_r(\Delta T/\nu) \exp(-E_r/RT) \quad (4)$$

To start the simulation, a saturated benzene monolayer is accommodated to reproduce the structure given in Figure 6c. The following sequence of steps is then followed: (1) The initial temperature is fixed at T_0 (250 K). (2) The temperature is increased by ΔT such that both P_d and P_r are much less than unity. The number of chemisorbed benzenes on the surface at this point is n . (3) A chemisorbed benzene molecule is randomly selected and values of P_d and P_r are calculated. A random number R is generated such as to be uniformly distributed in the range $0 < R < 1$. A molecule desorbs if $0 < R < P_d$, reacts if $P_d < R < P_d + P_r$ and remains unaffected otherwise. This step is repeated n times. (4) n is now set to $n - \Delta n$ where Δn is the total number of benzene molecules that have either desorbed or decomposed. (5) The cycle is repeated from step 2 until no benzene remains ($n = 0$).

Desorption spectra for smaller initial benzene coverages are simulated by desorbing sufficient benzene to attain the desired initial coverage after which the procedure described above is followed to simulate the spectrum.

The fit to the experimental spectra is obtained by trial and error until a visually satisfactory agreement is reached. The final simulations are displayed in Figure 7 which shows the simulated spectra for benzene desorption. The parameters used for the simulation are $\nu_d = \nu_r = 1 \times 10^7 \text{ s}^{-1}$, $E_{\text{ads}} = 101 \text{ kJ/mol}$, $W = -6.5 \text{ kJ/mol}$, $E_r^0 = 82 \text{ kJ/mol}$, and $V = 5 \text{ kJ/mol}$. Clearly the β and γ features of the experimental spectra are well reproduced,

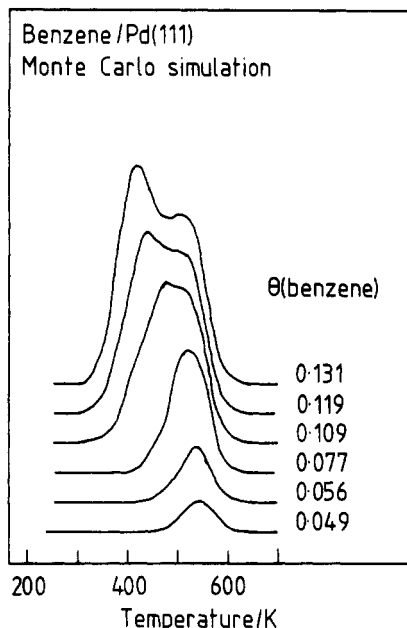


Figure 7. Results of a Monte Carlo simulation of the desorption of benzene from Pd(111) as a function of coverage.

in particular the observation that all adsorbed benzene for $\theta < 0.05$ thermally decomposes to desorb hydrogen (Figures 2 and 3) whereas it desorbs molecularly at higher coverages (Figure 3). This effect can be ascribed to the strong repulsive interactions between adjacent benzenes (6.5 kJ/mol) which facilitate desorption at higher coverages and to the effect of blocking of sites available for decomposition products. The spectra also clearly distinguish the presence of the β and γ states which are both adequately described by the incorporation of just nearest neighbor interactions.

It might be anticipated from the structural models displayed in Figure 6 that benzene overlayers on Pd(111) should exhibit an array of LEED patterns whereas none have been detected in the absence of coadsorbates.^{18,19,32,33} A possible explanation for this observation is that the benzene structures shown in Figure 6 nucleate randomly on the surface at out-of-phase (possibly 2-fold) sites. If the resulting out-of-phase islands are smaller than typical electron beam coherence lengths (~ 100 Å) they will therefore be invisible in LEED. It is possible that the boundaries between these domains may also act as nucleation sites for the formation of tilted benzene (see below). This phenomenon is being investigated further using Monte Carlo simulations of the adsorption kinetics. Note, however, that a $\sqrt{7} \times \sqrt{7}R$ 19.1° LEED structure has been observed for benzene on Ni(111) at 200 K corresponding to a coverage of 0.143^{20,21} (in good agreement with the value measured here). This ordered structure disappears on annealing to 300 K due to benzene desorption lowering the surface coverage to 0.09.

Tilted Benzene. Continued adsorption of benzene can now only be accommodated by tilting increasing numbers of molecules out of the surface plane to provide the necessary adsorption sites—this corresponds to the onset of desorption from the α state. This is in line with the experimental observation that the desorption energy associated with the α state is very substantially lower than that associated with the β and γ states, the latter being identified with flat-lying benzene. It is also consistent with the observation that adsorption into the α state is somewhat activated with a sticking probability which is more than an order of magnitude lower than the sticking probability into flat-lying states. We may rule out the possibility that the α state is due to the adsorption of a second layer of benzene molecules for the following reasons:

(1) The desorption energy of benzene multilayers is ~ 35 kJ/mol⁴ in good agreement with the enthalpy of sublimation of

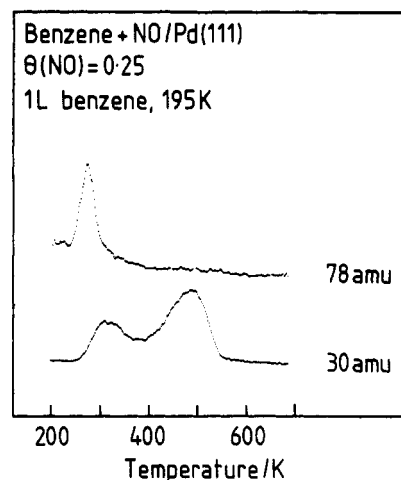


Figure 8. Thermal desorption spectrum obtained following a 1-langmuir benzene exposure to a NO precovered surface ($\theta(\text{NO}) = 0.25$) at 200 K showing the resulting 78 (benzene) and 30 (NO) amu signals.

benzene 44 kJ/mol;³⁵ the associated peak temperature is ~ 150 K. These values are significantly different to the corresponding α state values (280 K), and there is no reason to suppose that the properties of the third and subsequent layers should differ significantly from those of the second layer.

(2) The α state sticking probability is ~ 0.03 . Second layer condensation would be expected to occur with a sticking probability close to unity.

(3) The α state intensity saturates at a coverage of ~ 0.21 , whereas uptake into a condensed layer would proceed without saturation.

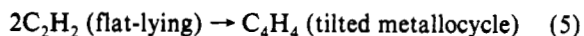
(4) There is direct spectroscopic evidence (NEXAFS¹⁰) which shows that in the coverage regime corresponding to α state desorption, these dense overlayers consist of molecules in which the molecular plane is tilted at $\sim 30^\circ$ with respect to the metal surface.

(5) It has been shown that compressed phases exhibiting only the α desorption state can be formed at relatively low coverages using NO as an inert spectator molecule¹¹ (see below).

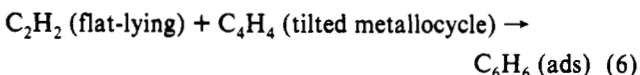
It has been shown previously that compressed phases can be formed at relatively low coverages using inert spectator molecules such as NO. For example, coadsorption of NO with acetylene results only in the low temperature (~ 280 K) benzene desorption state. The results of a similar experiment are displayed in Figure 8 which shows benzene and NO thermal desorption spectra obtained by exposing an NO-covered surface ($\theta(\text{NO}) = 0.25$) to 1.0 langmuir of benzene at 200 K. On clean Pd(111) this exposure leads to a benzene coverage of 0.13 and the appearance of the β and γ states in thermal desorption (Figure 3). However, as illustrated in Figure 8, compression of this benzene layer by NO leads exclusively to the formation of the tilted α state which appears at ~ 280 K. The interaction between coadsorbed NO and benzene is confirmed by the NO desorption spectrum which shows a peak at ~ 315 K in addition to the molecular desorption state at ~ 490 K, a desorption state which is observed for this coverage of NO on clean Pd(111). No hydrogen desorption is detected from this surface in accord with the observed destabilization of the benzene overlayer, i.e., no benzene decomposes. Reversing the order of desorption leads to some compression of the benzene overlayer as evidenced by a slight increase in the intensity of the α state. This effect is, however, not as pronounced as in the case where acetylene compression layers are formed by NO postdosing,¹¹ presumably reflecting the stronger adsorption of benzene on Pd(111) than acetylene. Work by Netzer et al.³⁵ on the (110) surface of palladium led these workers to propose a benzene overlayer that was tilted at 10 – 20° following room temperature adsorption. This was, however, ascribed to the effect

of accommodation to the microscopically rough (110) surface rather than to surface crowding.

Finally, it is of interest to compare kinetic results for benzene adsorbed directly onto palladium(111) with those of benzene formed reactively from acetylene. The trimerization reaction pathway can be summarized as follows:



Benzene is formed by the reaction of the C_4 intermediate with acetylene according to



The C_4 formation pathway is likely to be rather fast since grafting C_4 species directly onto the surface by $\text{C}_4\text{H}_4\text{Cl}_2$ decomposition followed by acetylene adsorption produces an identical thermal desorption spectrum as when dosing acetylene alone. Acetylene saturates at 200 K on Pd(111) at a coverage of 0.46¹ which is equivalent to a benzene coverage of 0.15. This indicates that any benzene that is reactively formed on Pd(111) from acetylene is crowded and must therefore adopt a tilted configuration and therefore desorb at ~280 K. Such a model therefore successfully accounts for the observation of the low temperature desorption state in the spectrum of reactively formed benzene. As the crowding is relieved on the surface, either by the desorption of excess acetylene or by conversion of surface species into vinylidene,¹ remaining surface benzene may adopt a flat lying geometry and consequently desorbs at higher temperatures.

Conclusions

Benzene adsorbs onto Pd(111) at 200 K with an initial sticking probability of unity, the overlayer saturating at a coverage of ~0.13. This coverage corresponds to a close-packed layer of benzene molecules oriented with their molecular planes parallel to the surface. A structural model has been developed for this layer, and the thermal desorption of benzene from this layer is successfully reproduced using Monte Carlo simulations. Results of the simulation suggest that the heat of adsorption of flat lying benzene on palladium is ~101 kJ/mol. There are a strong repulsive interactions between neighboring benzene molecules and this interaction successfully accounts for the benzene desorption spectrum and the thermal dehydrogenation of chemisorbed benzene at low coverages.

Further adsorption occurs with a much lower sticking probability up to a saturation coverage of ~0.22, the additional benzene desorbing at ~280 K. This, along with results of experiments where the benzene overlayer is compressed using

NO indicates that this state is due to the presence of a tilted benzene layer.

References and Notes

- (1) Tysoe, W. T.; Nyberg, G. L.; Lambert, R. M. *Surf. Sci.* **1983**, *135*, 128.
- (2) Sesselman, W.; Woratschek, B.; Ertl, G.; Küppers, J.; Haberland, H. *Surf. Sci.* **1983**, *130*, 245.
- (3) Gentle, T.; Muetterties, E. L. *J. Phys. Chem.* **1983**, *87*, 245.
- (4) Patterson, C. H.; Lambert, R. M. *J. Phys. Chem.* **1988**, *92*, 1266.
- (5) Patterson, C. H.; Lambert, R. M. *J. Am. Chem. Soc.* **1988**, *110*, 6871.
- (6) Patterson, C. H.; Mundenar, J. M.; Timbrell, P. Y.; Gellman, A. J.; Lambert, R. M. *Surf. Sci.* **1989**, *208*, 93.
- (7) Gellman, A. J. *Langmuir* **1991**, *7*, 827.
- (8) Ormerod, R. M.; Lambert, R. M. *Catal. Lett.* **1990**, *6*, 121.
- (9) Ormerod, R. M.; Lambert, R. M. *J. Chem. Soc., Chem. Commun.* **1990**, *20*, 1421.
- (10) Hoffmann, H.; Zaera, F.; Ormerod, R. M.; Lambert, R. M.; Wang, L. P.; Tysoe, W. T. *Surf. Sci.* **1990**, *232*, 259.
- (11) Ormerod, R. M.; Lambert, R. M. *Surf. Sci.* **1990**, *225*, L20.
- (12) Ormerod, R. M.; Badderley, C. J.; Lambert, R. M. *Surf. Sci.* **1991**, *259*, L709.
- (13) Ormerod, R. M.; Lambert, R. M. *J. Phys. Chem.* **1992**, *96*, 8111.
- (14) King, D. A.; Wells, M. G. *Proc. R. Soc. (London)* **1974**, *A339*, 245.
- (15) Summers, R. L. NASA Technical Note TN D-5285; National Aeronautics and Space Administration: Washington, DC, 1969.
- (16) Conrad, H.; Ertl, G.; Latta, E. E. *Surf. Sci.* **1974**, *41*, 435.
- (17) Redhead, P. A. *Vacuum* **1980**, *12*, 203.
- (18) Netzer, F. P.; Mack, J. U. *J. Chem. Phys.* **1983**, *79*, 1017.
- (19) Wadill, G. D.; Kesmodel, L. L. *Phys. Rev. B* **1985**, *31*, 4940.
- (20) Huber, W.; Steinruck, H. P.; Pache, T.; Menzel, D. *Surf. Sci.* **1989**, *217*, 103.
- (21) Huber, W.; Zebisch, P.; Bornemann, T.; Steinruck, H. P. *Surf. Sci.* **1991**, *258*, 16.
- (22) Johnson, A. L.; Muetterties, E. L.; Stöhr, J. *J. Am. Chem. Soc.* **1983**, *105*, 7183.
- (23) Somers, J.; Bridge, M. E.; Lloyd, D. R.; McCabe, T. *Surf. Sci.* **1987**, *181*, L167.
- (24) Ogletree, D. F.; Van Hove, M. A.; Somorjai, G. A. *Surf. Sci.* **1987**, *183*, 1.
- (25) Van Hove, M. A.; Lin, R.; Somorjai, G. A. *Phys. Rev. Letts.* **1983**, *51*, 778.
- (26) Koel, B. A.; Crowell, J. E.; Mate, C. M.; Somorjai, G. A. *J. Phys. Chem.* **1984**, *88*, 1988.
- (27) Neumann, M.; Mack, J. U.; Bertel, E.; Netzer, F. P. *Surf. Sci.* **1985**, *155*, 629.
- (28) Netzer, F. P.; Rosina, G.; Bertel, E.; Saalfeld, H. *Surf. Sci.* **1987**, *184*, L397.
- (29) Mack, J. U.; Bertel, E.; Netzer, F. P. *Surf. Sci.* **1985**, *159*, 265.
- (30) Sales, J. L.; Zgrablich, G. *Surf. Sci.* **1987**, *187*, 1.
- (31) Heras, J. M.; Velasco, A. P.; Viscido, L.; Zgrablich, G. *Langmuir* **1991**, *7*, 1124.
- (32) Ohtani, H.; Van Hove, M. A.; Somorjai, G. A. *J. Phys. Chem.* **1988**, *92*, 3974.
- (33) Ohtani, H.; Bent, B. E.; Mate, C. M.; Van Hove, M. A.; Somorjai, G. A. *Appl. Surf. Sci.* **1988**, *33/34*, 254.
- (34) Weast, R. C.; Selby, S. M., Eds. *Handbook of Chemistry and Physics*; Chemical Rubber Co.: Cleveland, 1967.
- (35) Netzer, F. P.; Rangelov, G.; Rosina, G.; Saalfeld, H. B.; Neumann, M.; Lloyd, D. R. *Phys. Rev. B* **1988**, *37*, 10399.